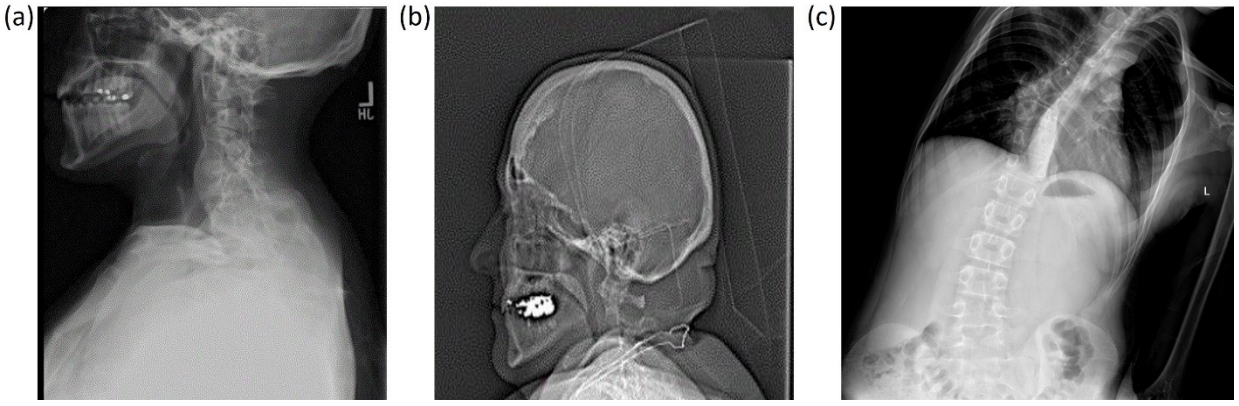

Supplemental Figure 1. Radiographic illustration of proband vertebral malformations. (a) Proband 1: x-ray showing fused C4-C5 cervical vertebrae in a 46 year old female (b) Proband 2: CT scan showing fused C3-C5 cervical vertebrae in a 31 year old male. (c) Proband 3: 20-year old male with congenital scoliosis and hemivertebra of T9 demonstrated by x-ray.

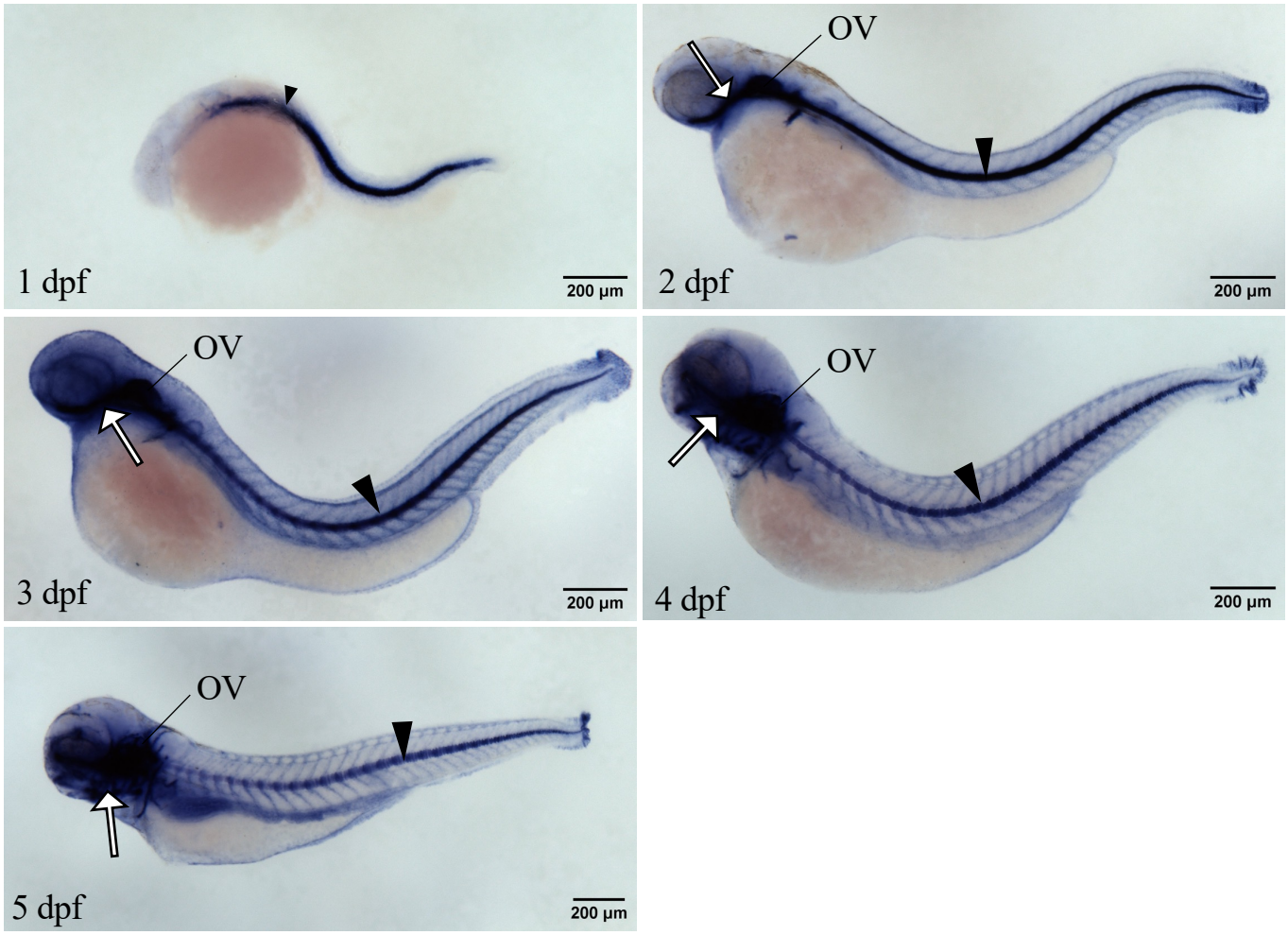

Supplemental Figure 2. Whole mount RNA *in situ* hybridization demonstrating the spatiotemporal expression pattern of *col11a2* in zebrafish embryos from 1-5dpf. *col11a2* is expressed in the developing notochord (arrowheads) and craniofacial cartilage (white arrows), consistent with a role in skeletal development.

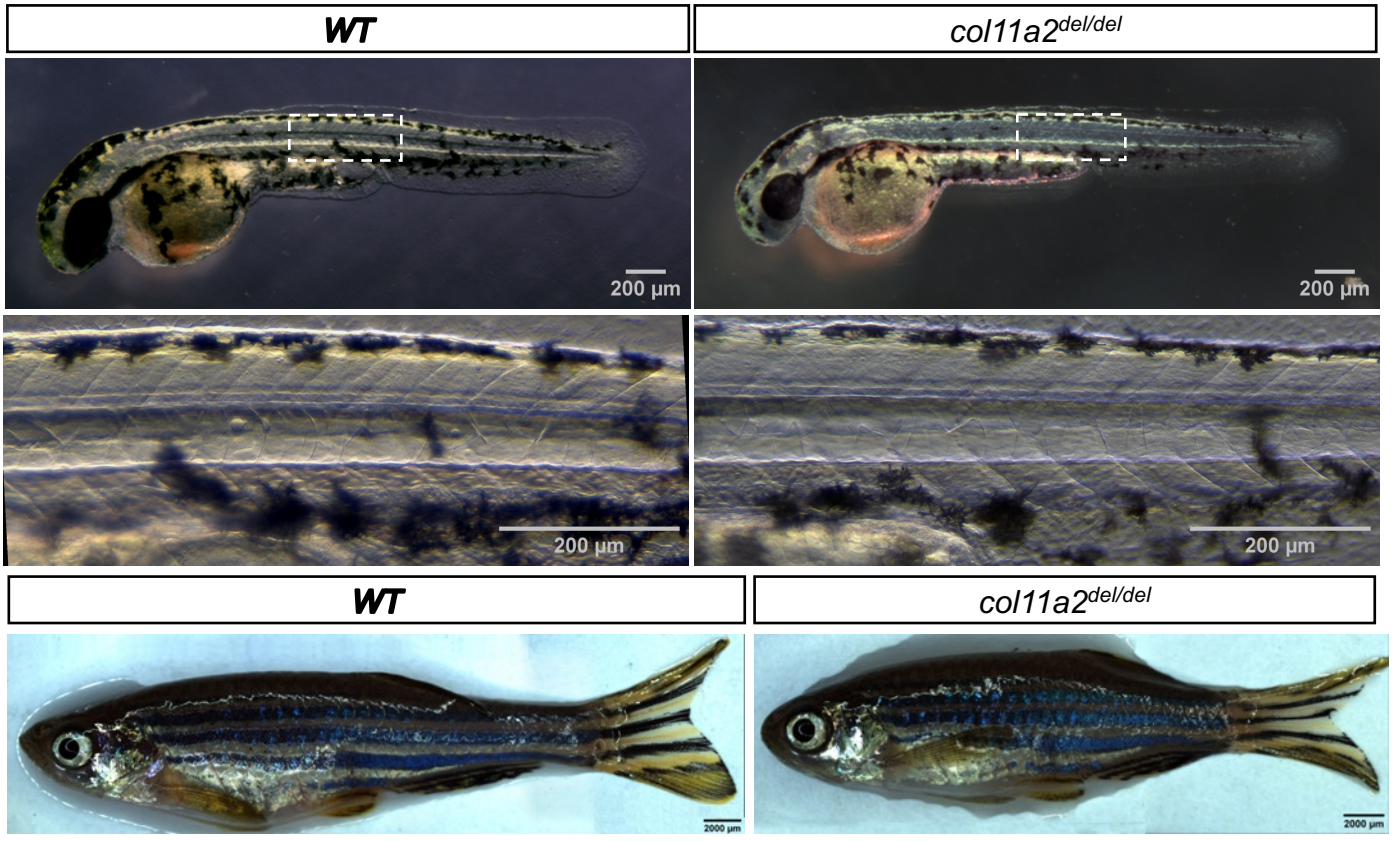

Supplemental Figure 3. *col11a2*$^{del/del}$ mutant animals appear morphologically normal. Live, whole-mount images of wildtype (left) and *col11a2*$^{del/del}$ mutant (right) fish at 48hpf embryonic (top) and adult (bottom) stages. 2dpf *col11a2*$^{del/del}$ embryos do no exhibit obvious morphological defects. Vertebral fusions in adult *col11a2*$^{del/del}$ animals do not result in axial curvatures, but mutant fish do appear shorter in length than wildtype, and exhibit a craniofacial defect.

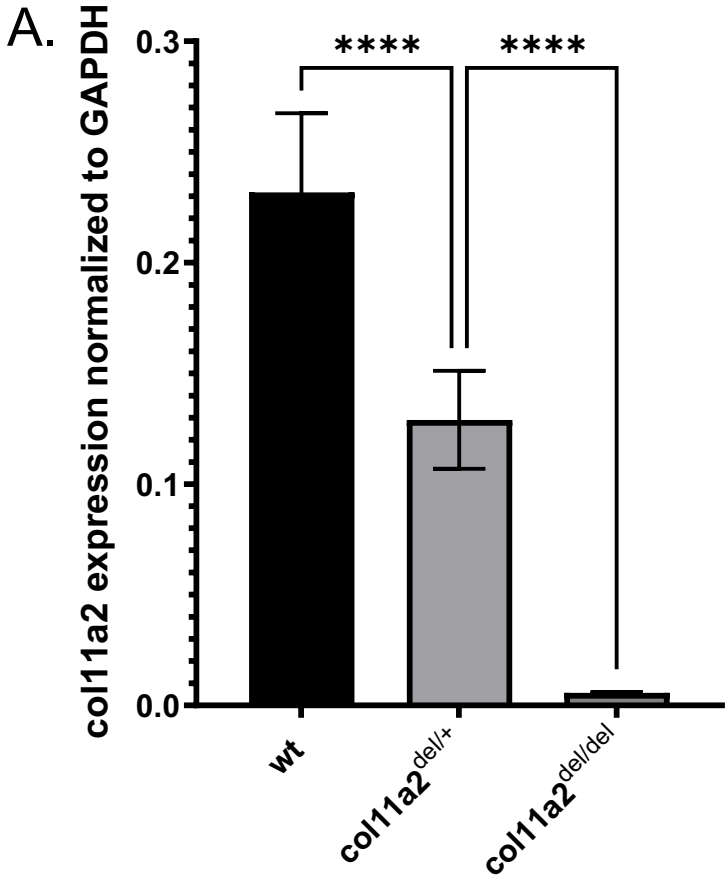

Supplemental Figure 4. RT-qPCR analysis of *col11a2* expression levels in 2dpf embryos. A. *col11a2* expression in *col11a2*$^{del/+}$ embryos is approximately half of of wildtype expression levels and is almost undetectable in *col11a2*$^{del/del}$ mutant embryos. B. No significant differences in *col11a2* expression are observed between wildtype and patient-mutation bearing *col11a2* transgenic lines. All expression levels were normalized to *gapdh* expression within the same sample. Each genotype included three biological replicates, with three technical replicates of each. Error bars represent standard deviation and significance was calculated by one-way ANOVA with Dunnett's *post hoc* test. * p<0.05, ** p<0.01, *** p<0.001, **** p<0.0001.

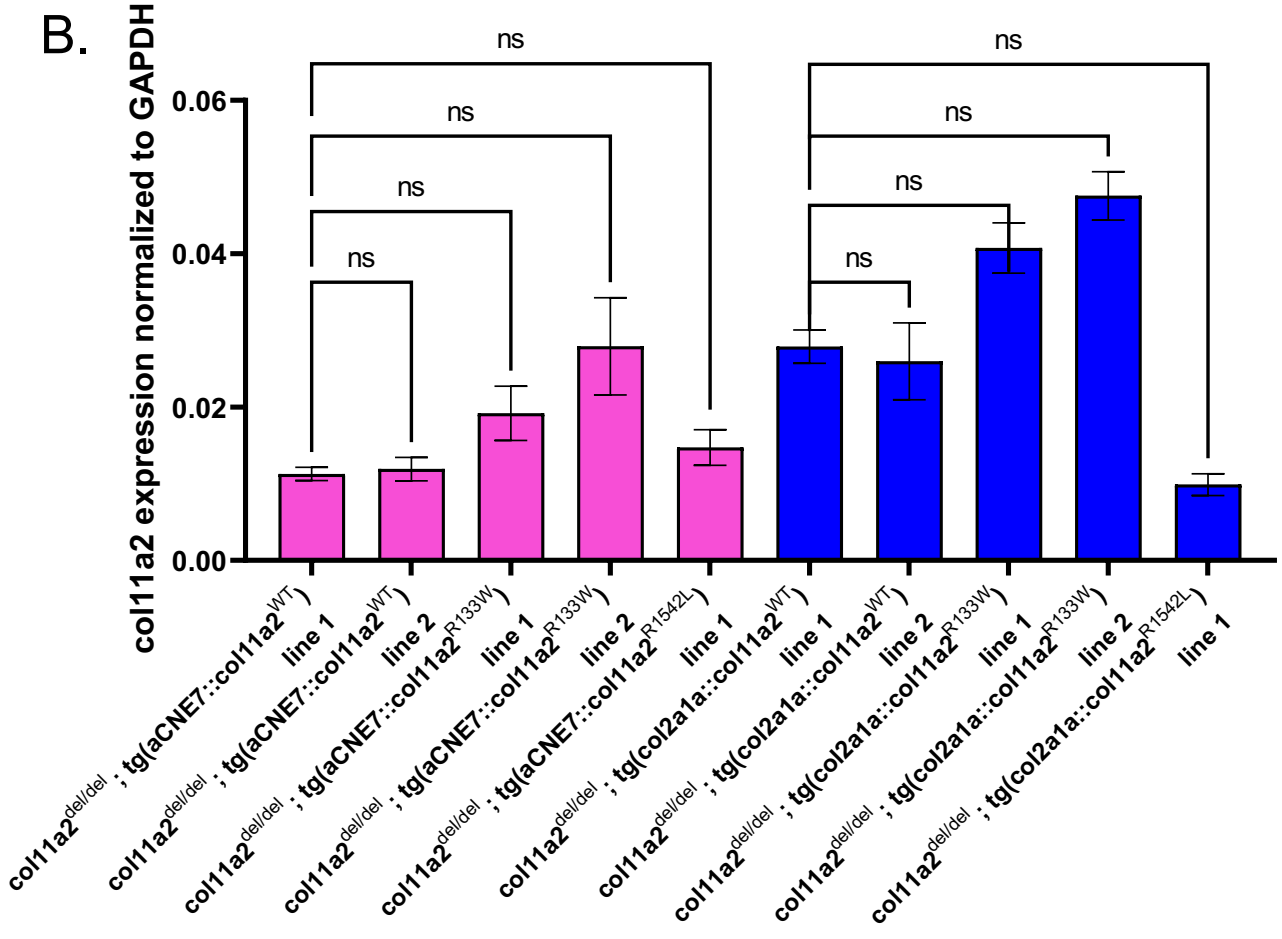

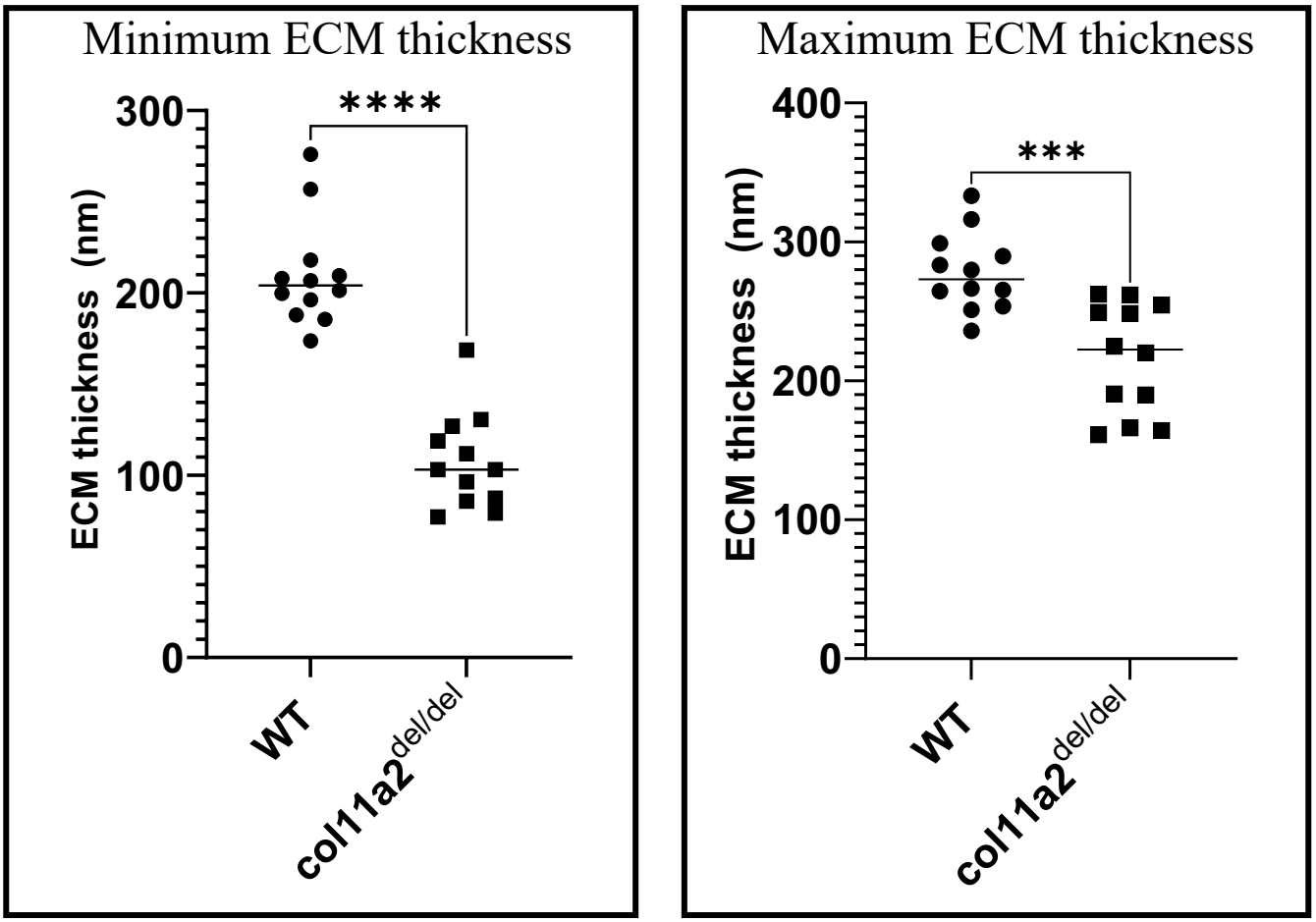

Supplemental Figure 5. Notochord ECM is significantly thinner in *col11a2*$^{del/del}$ mutant embryos. Quantification of notochord ECM thickness from TEM images of 2 dpf wildtype and *col11a2*$^{del/del}$ mutant embryos. Both the minimum thickness (A) and maximum thickness (B) are significantly reduced in *col11a2*$^{del/del}$ embryos. n=6 for each genotype, thickness measured on both lateral sides of TEM notochord cross-sections. Significance calculated using Student's t-test. * $p<0.05$, ** $p<0.01$, *** $p<0.001$, **** $p<0.0001$.

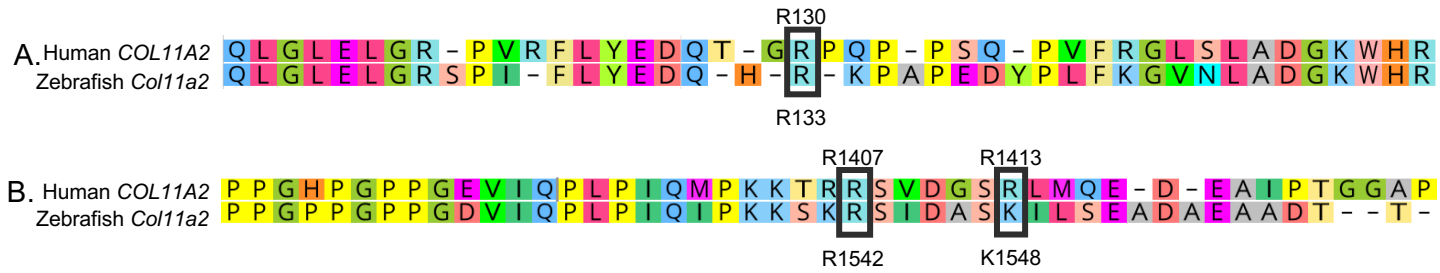

Supplemental Figure 6. Partial alignment of the human and zebrafish Col11a2 proteins. Panel A shows the alignment of the early part of the protein, highlighting conserved human R130 and zebrafish R133 residues. Panel B shows the alignment of the C terminal end of the triple helix domain. Human R1407 is conserved in the fish and aligns with R1542. R1413 in the human protein is not conserved in zebrafish.